

On the Selectivity in the Synthesis of 3-Fluoropiperidines Using BF_3 -Activated Hypervalent Iodine Reagents

Radoslav Z. Pavlović,^{a,b*} Tatjana J. Kop,^b Marko Nešić,^{c‡} Olivera Stepanović,^{d‡} Xiuze Wang,^{a,†} Nina Todorović,^b Marko V. Rodić,^e and Biljana M. Šmit^{f*}

Dedicated to Dr. Mira S. Bjelaković and Prof. T. V. RajanBabu.

^aDepartment of Chemistry & Biochemistry, The Ohio State University, 100 West 18th Avenue, Columbus, Ohio 43210, United States

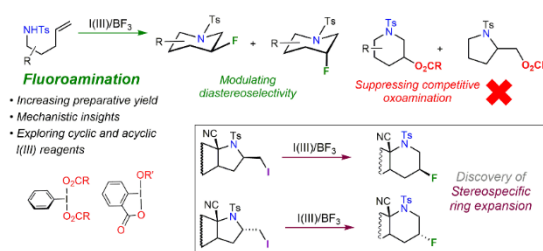
^bUniversity of Belgrade, Institute of Chemistry, Technology and Metallurgy, Department of Chemistry, Njegoševa 12, 11000 Belgrade, Serbia

^cRoger Adams Laboratory, Department of Chemistry, University of Illinois at Urbana-Champaign, Urbana, Illinois 61801, United States

^dLaboratory of Organic Chemistry, ETH Zürich, Vladimir-Prelog-Weg 3, 8093 Zürich, Switzerland

^eUniversity of Novi Sad, Faculty of Sciences, Trg Dositeja Obradovića 3, 21000 Novi Sad, Serbia

^fUniversity of Kragujevac, Institute for Information Technologies, Department of Science, Jovana Cvijića bb, 34000 Kragujevac, Serbia



Abstract:

Fluorinated piperidines find wide applications most notably in the development of novel therapies and agrochemicals. Cyclization of alkenyl *N*-tosylamides promoted by BF_3 -activated aryl iodine(III) carboxylates is an attractive strategy to construct 3-fluoropiperidines but it suffers from selectivity issues arising from competitive oxoaminations and inability to easily modulate the reactions diastereoselectivity. Herein we report an itemized optimization of the reaction conditions carried out on both cyclic and acyclic substrates and outline the origins of substrate- and reagent-based stereo-, regio- and chemoselectivity. Extensive mechanistic studies encompassing multinuclear NMR spectroscopy, deuterium labelling, rearrangements on stereodefined substrates, and careful structural analyses (NMR and X-ray) of the reaction products are performed. This revealed the processes and interactions crucial for achieving controlled preparation of 3-fluoropiperidines using I(III) chemistry and has provided an advanced understanding of the reaction mechanism. In brief, we propose that BF_3 -coordinated I(III) reagents attack C=C to produce the corresponding iodonium(III) ion which then undergoes diastereodetermining 5-exo-cyclization. Transiently formed pyrrolidines with exocyclic σ -alkyl-I(III) moiety can further undergo aziridinium ion formation or reductive ligand coupling processes, which dictates the final product's ring size but also the chemoselectivity. Importantly, selectivity of the reaction depends on the nature of the ligand bound to I(III) and the

presence of electrolytes such as TBABF₄. Reported findings will facilitate the usage of ArI(III)-dicarboxylates in reliable construction of fluorinated azaheterocycles.

Introduction

The increasing need for construction of complex and diverse organic molecules represents a grand challenge for the synthetic community.^{1–4} Accordingly, the development of highly predictable, efficient, and selective transformations is in high demand due to their central role in finding new life-changing molecules (pharmaceuticals, agrochemicals and materials).^{5,6} The paramount importance lies in questioning and re-examining reaction mechanisms since it expands the fundament of chemical space with new reaction intermediates and transition states (TS[‡]), which is the foundation for addressing the abovementioned challenges.⁷ For instance, the impact of inspecting the reaction mechanism is easily recognizable in the discovery of Schrock and Grubbs catalysts, which were inspired by Chauvin's proposal of the formation of a metal-carbene intermediate during olefin metathesis reactions.⁸

Saturated azaheterocycles appear in numerous biologically⁹ and pharmacologically^{10,11} relevant structures. The piperidine moiety, as the most prevalent, is found among 59% FDA-approved small-molecule therapeutics that contain at least one azaheterocycle.¹² On the other hand, the presence of C—F bonds is highly desirable in pharmaceuticals, where 20% of all marketed drugs possess at least one fluorine atom.^{13,14} It is well established that fluorination of parent test compounds delivers candidates with improved bioavailability, metabolic stability and lipophilicity (Figure 1A).^{13–19} Importantly, C—F bonds can be engaged in numerous non-covalent interactions (Figure 1B), which are relevant for achieving bioactivity.²⁰

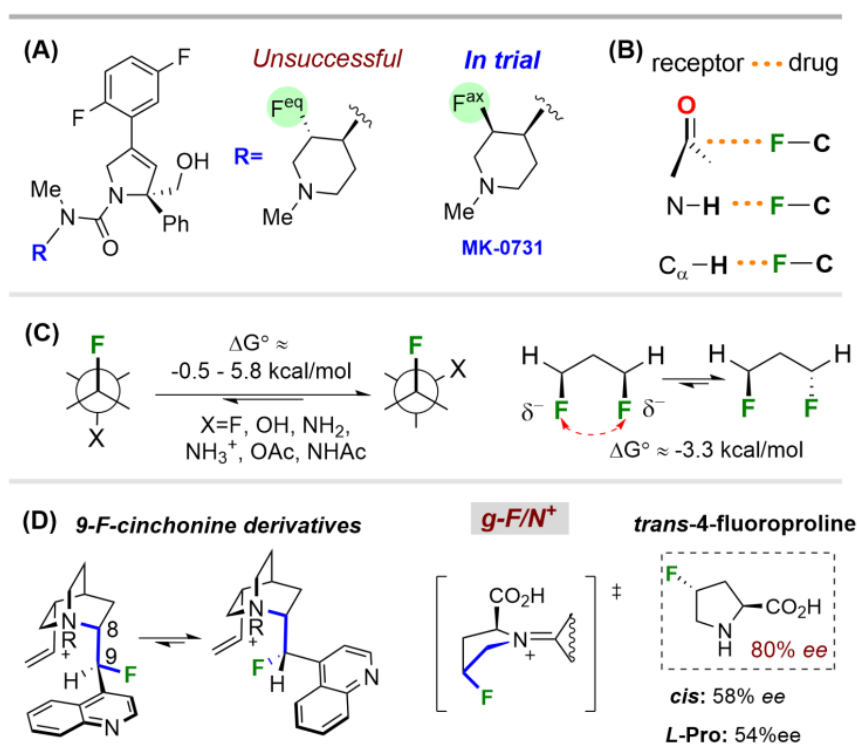


Figure 1. Benefits of installing stereodefined C—F bond seen in improving metabolic stability of a drug candidate (A), introducing new specific noncovalent drug-receptor interactions (B) and inducing the conformational bias (C), which is useful for new catalyst and drug design (D).

Besides explicit ligand-receptor non-covalent interactions in which C—F bonds can be engaged, such bonds are highly useful in biasing conformational ensembles of flexible alkyl chains (Figure 1C), which is extremely relevant for catalytic synthetic methods,^{16,17} as well as in drug development (Figure 1D).¹⁸ Accordingly, predictive, effective and modular methodologies for introducing stereodefined C—F bonds are strongly desired.^{19,21} In this light, the Glorius group reported a highly diastereoselective Rh-catalyzed transformation of (poly)fluorinated pyridines into all-*cis*-(poly)fluorinated piperidines.^{21a} On the other hand, Liu's group developed highly regioselective alkene fluoroamination protocols utilizing high-valent palladium chemistry for the preparation of β -fluorinated piperidines^{22,23} and pyrrolidines (Figure 2).²⁴

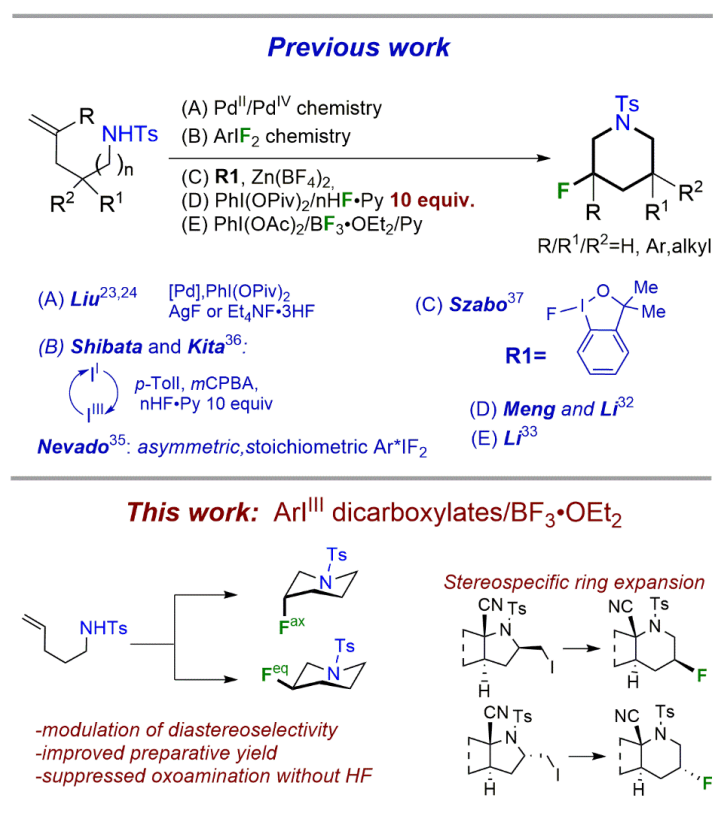


Figure 2. Current reactions available for the preparation of 3-fluoropiperidines utilizing Pd^{II}/Pd^{IV} and I^{III} chemistry.

Given the power of intramolecular formation of C—N bond in constructing azaheterocycles,²⁵ throughout the prior decade we have been exploring organoselenium chemistry in cyclizing alkenes bearing hydantoins. We have noticed that organoselenium promoted cyclizations of such substrates give pyrrolidine type fused bicyclic products.²⁶⁻²⁸ Nowadays, tremendous effort is being put towards the development and understanding of metal-free hypervalent iodine promoted reactions, due to the reagent's low toxicity, commercial availability, reusability, convenient structural modifications, mild reaction conditions, and its potential to be adapted to work under catalytic conditions (I(I)/I(III)).²⁹⁻³⁴ Four sets of reaction conditions which include I(III) have been reported hitherto for constructing 3-fluoropiperidines (Figure 2, B-E).^{32,33,35-37} The last set of conditions outlined in Figure 2E³³ () intrigued us for three reasons: 1) utilization of commercially available and stable oxidant (Ar(I) stability: AcO>F), 2) usage of BF₃·Et₂O as an activator and source of fluoride, which is complementary to catalytic Pd(II)/Pd(IV) and I(I)/I(III) chemistry, where excess of AgF or amine·HF is required (incompatible with silyl protecting groups³⁸⁻⁴⁰) and

3) relatively short reaction times (potential application in making ^{18}F -labeled molecules for PET).⁴¹ Herein, we wish to report new conditions for fluoroaminations of unactivated alkenes with an updated mechanistic model, as well as crucial substrate and reagent related factors in controlling chemo-, regio- and diastereoselectivity of this transformation (Figure 2, bottom). In addition, we report stereospecific rearrangements of *N*-tosyl-2-iodomethylpyrrolidines in the presence of $\text{BF}_3 \cdot \text{Et}_2\text{O}/\text{AR1-4}$ which enables the rapid construction of 3-fluorinated azaheterocycles (room temperature, reaction time < 5 min).

Results and Discussion

To gain deeper insight into the processes and interactions underlying aryliodine(III)-dicarboxylate promoted fluorocyclizations, we submitted **1** to reaction conditions similar to the ones already reported by Li^{33} to find that only 9% of **2'-F** product is obtained (Figure 3, entry 1).

| Entry | Reagent | LA | Additive | 2-L | 2'-L | 2'-F |
|-------|------------------|----------------------------------|---------------------------|----------------|-----------------|---------|
| 1 | AR1 ^a | $\text{BF}_3 \cdot \text{OEt}_2$ | | 12 | 78 | 10 [9] |
| 2 | AR1 ^b | $\text{BF}_3 \cdot \text{OEt}_2$ | | 10 | 70 | 20 |
| 3 | AR2 ^b | $\text{BF}_3 \cdot \text{OEt}_2$ | | 3 | 22 | 75 [71] |
| 4 | AR1 ^b | $\text{BF}_3 \cdot \text{OEt}_2$ | TBAPF ₆ 10 eq. | 8 | 81 | 11 |
| 5 | AR1 ^b | $\text{BF}_3 \cdot \text{OEt}_2$ | AgSbF ₆ 3 eq. | 8 | 77 | 15 |
| 6 | AR1 ^b | $\text{BF}_3 \cdot \text{OEt}_2$ | TBABF ₄ 10 eq. | 7 | 39 | 54 |
| 7 | AR1 ^b | $\text{BF}_3 \cdot \text{OEt}_2$ | TBABF ₄ 20 eq. | 6 | 31 | 63 |
| 8 | AR1 ^b | $\text{BF}_3 \cdot \text{OEt}_2$ | TBABF ₄ 50 eq. | 3 | 23 | 74 [71] |
| 9 | AR1 ^b | TrBF ₄ | | 13 | 76 | 11 |
| 10 | CR1 ^c | $\text{BF}_3 \cdot \text{OEt}_2$ | TBABF ₄ 50 eq. | 1 | 11 ^d | 88 [85] |
| 11 | CR2 ^c | $\text{BF}_3 \cdot \text{OEt}_2$ | TBABF ₄ 50 eq. | 4 ^e | 35 ^e | 61 |

^a $\text{BF}_3 \cdot \text{OEt}_2$ (3 equiv) added in one portion into the solution of **1** and AR1; **isolated yield [%]**; ^bAR1/2 added portionwise to the solution of **1** and LA (3 equiv)/additive; ^cCR1/2 added to **1** and $\text{BF}_3 \cdot \text{OEt}_2$ /additive in one portion; ^dL=2-iodo-benzoate; ^eL= OAc/2-iodobenzoate~1:1.

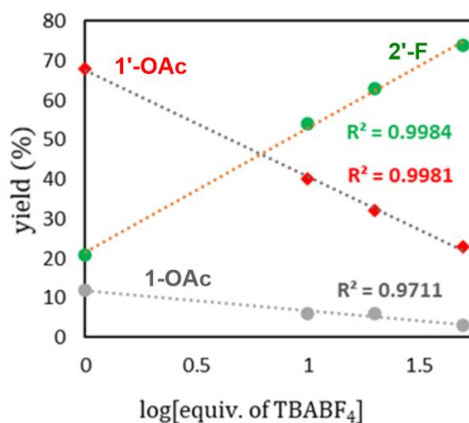
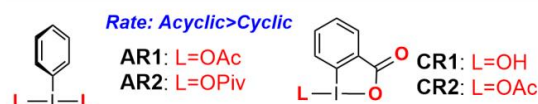
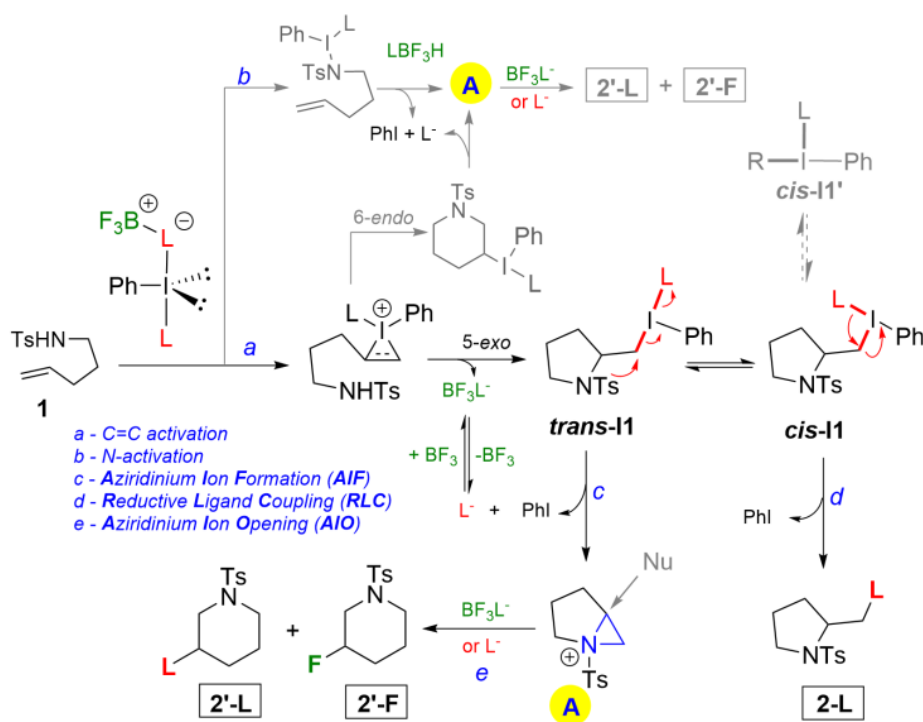


Figure 3. The influence of the reagent, reaction setup and the presence of TBABF₄ (plot) on the fluoroamination of **1**. Product distribution was determined by ^1H NMR spectroscopy (see SI for details and figure S2 for all tested ligands).

^1H NMR spectroscopy showed that **1** was fully converted immediately after the addition of $\text{BF}_3 \cdot \text{Et}_2\text{O}$ (~ 1 min), but acetoxyated products (**2'-OAc** and **2-OAc**) were prevalent. Interestingly, the yield of **2'-F** doubled (20%) when the CH_2Cl_2 -solution of **AR1** was added dropwise to the solution of **1** and $\text{BF}_3 \cdot \text{Et}_2\text{O}$ (Figure 3, entry 2). We were extremely excited to find that carboxylate ligands attached to I^{III} strongly influence the chemoselectivity of the reaction, with pivalate giving the highest yield of **2'-F** (Figure 3, entry 3) concomitantly reducing the yield of the 5-*exo* product **2-L**. Reactions with reagent **AR1** (i.e. PIDA) in the presence of different additives and Lewis acids were performed (Figure 3, entries 4-9). Fascinatingly, in the presence of BF_4^- (≥ 10 equiv.) the yield of **2'-F** increases significantly (Figure 3, entries 6-8), while PF_6^- (Figure 3, entry 4) and SbF_6^- (Figure 3, entry 5) did not show such effect. The linear dependence between the yields of reaction products and the logarithm of TBABF_4 concentration indicates that BF_4^- can directly deliver the fluoride (Figure 3, plot). Using tropylium tetrafluoroborate (TrBF_4) produced less **2'-F** (Figure 3, entry 9) in comparison to $\text{BF}_3 \cdot \text{Et}_2\text{O}$. These experiments suggest that *in situ* formed BF_3L^- species are likely delivering the nucleophilic fluoride, with the nucleophilic character decreasing in the series: $\text{BF}_3\text{L}^- > \text{BF}_4^- > \text{SbF}_6^- > \text{PF}_6^-$. Plausibly, a larger number of F-ligands bound to the central atom, as well as its higher electronegativity, reduce the overall nucleophilicity of the anion. In contrast to **AR1-2** (Figure 3 and Table S1), the reactions with cyclic reagents **CR1-2** are much slower. However, reagent **CR1** delivered the desired product **2'-F** in the highest yield (Figure 3, entry 10, 85%). Interestingly more products of competitive oxoamination (**2-L** and **2'-L**) were observed with **CR2** compared to **CR1** (Figure 3, entry 11).



Scheme 1. The proposed mechanism of the $\text{I}^{\text{III}}/\text{BF}_3 \cdot \text{Et}_2\text{O}$ promoted cyclization of alkenyltosylamide **1** (black). Other possible pathways, such as *N*-activation (b) or direct 6-*endo* cyclization, are colored gray. The low population of the *cis-I1'* state is postulated to arise due to the less favorable *trans*-arrangement of R/Ph.^{49,50}

Inspired by prior reports, the mechanism shown in Scheme 1 was postulated to account for the regio- and chemoselectivity of the reaction. First, BF_3 -coordinated I^{III} -dicarboxylate ($\text{PhIL}_2 \cdot \text{BF}_3$)⁴² reacts with substrate **1** to promote C=C and/or *N*-activation.^{35,43} The corresponding iodiranium(III) intermediates produce **I1** via a favorable

5-*exo* ring closure.⁴⁴ This σ -alkyl I^{III} species exists in the form of interconvertible⁴⁵ *trans*- and *cis*-**11** isomers. The *trans*-(σ -alkyl)/L relationship in **11** facilitates aziridinium ion formation (AIF), while the *cis*-(σ -alkyl)/L setup enables reductive ligand coupling (RLC). Since no external nucleophile participates in the RLC, 5-*exo* products (**2-L**) are exclusively oxoaminated alkenes. However, 6-*endo* products are formed with various chemoselectivities (**2'-F/2'-L**), which can be reasoned through highly regioselective aziridinium ion (**A**) opening (AIO) with either F- or O-nucleophiles (Scheme 1). Finally, the observed suppression of **2-L** type products with the addition of electrolytes (TBABF₄, Figure 3) is in agreement with modulation of the electrostatic potential favoring the AIF-process.^{46–48} However, at this stage the other mechanistic possibilities, such as *N*-activation (*b* in Scheme 1) or direct 6-*endo* cyclization, could not be ruled out.

Direct characterization of the proposed I(III)-intermediates was unfeasible due to their kinetic invisibility, which aligns with prior reports on similar chemistry. However, we were fortunate to discover that cyclopentane (**3a**) and cyclohexane (**3b**) based substrates show rather dissimilar outcomes in the ring forming processes in mechanistically well-established electrophile-promoted nucleophilic cyclizations (EPNC, Figure 4A and S17-18).⁴⁴ For example, the iodocyclization reactions of the two substrates conducted under analogous conditions gave rather different conversion efficiency and product distribution (Figure 4A).

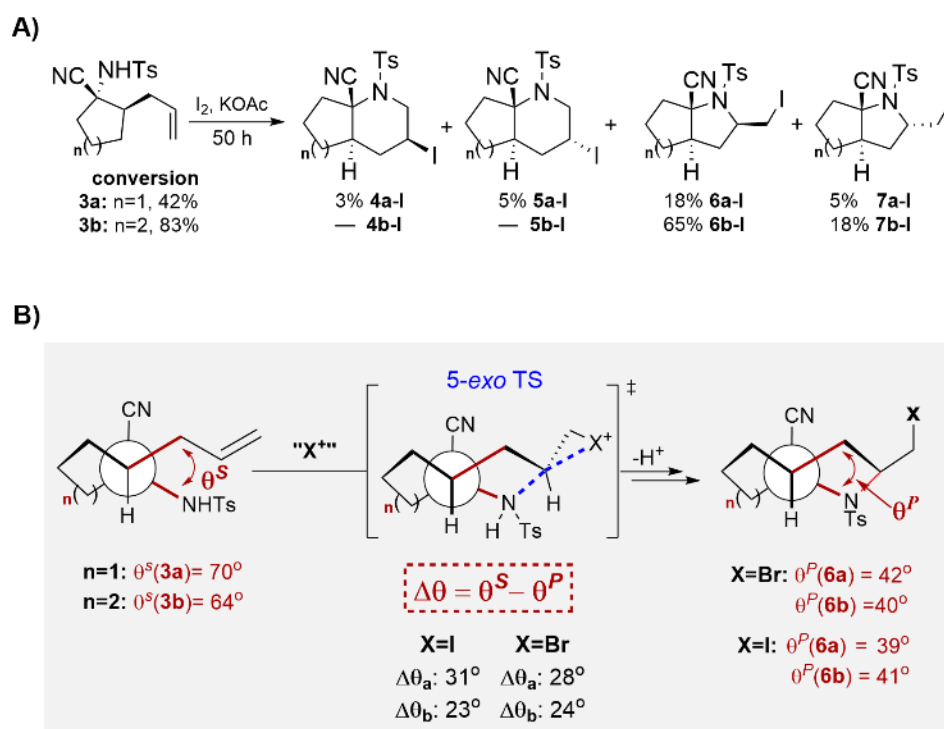


Figure 4. (A) Intramolecular aminoiodination reactions of substrates **3a-b**. Importantly, the notation **a** and **b** are used to describe the cyclopentane (**3a**) and cyclohexane (**3b**) skeleton in the substrates and the corresponding products. (B) The angle θ measured from the structural models of **3a**, **3b**, **6a-I**, **6a-Br**, **6b-Br**, **6b-Br** obtained via X-ray diffraction revealed $\Delta\theta(\mathbf{3a}) > \Delta\theta(\mathbf{3b})$ (this indicates a more challenging pyrrolidine ring closure for the **3a** system).

To further understand this observation, we submitted **6a/b-I** to the iodocyclization reaction conditions to find that they do not transform neither into **4a/b-I** nor the corresponding starting materials. This experiment suggests that a plausible ring enlargement (**6a/b-I** \rightarrow **4a/b-I**) is not an operative pathway and that the reaction is under kinetic control. Bearing in mind kinetic control of the reaction, much higher yield of the iodocyclization products obtained

starting from **3b** in comparison to **3a** is a clear evidence that the kinetic barriers (ΔG^\ddagger) for the corresponding ring closure processes are higher for cyclopentane-based substrate **3a**. Lastly, the product distributions obtained in the reactions shown in Figure 4A suggest that the difference in the corresponding 5-*exo* and 6-*endo* transition states (TS^\ddagger) energies must be much higher in the case of **3b** relative to **3a** (i.e., $\Delta G_{6-endo}^\ddagger(\mathbf{3a})/\Delta G_{5-exo}^\ddagger(\mathbf{3a}) < \Delta G_{6-endo}^\ddagger(\mathbf{3b})/\Delta G_{5-exo}^\ddagger(\mathbf{3b})$).

The finding that the two substrates differing only in a single methylene unit of their cycloalkane rings can react so differently was extremely intriguing and highly motivated us to develop an experimental approach based upon single crystal X-ray diffraction, to probe the structural origin of the dissimilarity in the reactivity of **3a** and **3b**. By performing a comparative analysis of the torsional angles θ (Figure 4B) in the two substrates **3a-b** (θ^S) and their 5-*exo* halocyclization products **6a-X** and **6b-X** (θ^P) we found that the angle change ($\Delta\theta(\mathbf{3a/b})$) occurring along **3a/b** \rightarrow **6a/b** pyrrolidine ring closure paths is rather different for the two systems (Figure 4B). The lower conversion of **3a** compared to **3b** (Figure 4A) and the measured $\Delta\theta(\mathbf{3a}) > \Delta\theta(\mathbf{3b})$ are in strong positive correlation. Therefore, we reasoned that larger structural deformation is required for cyclopentane-based substrate **3a** to undergo 5-*exo* processes relative to **3b**. We recognized this dramatic difference in reactivity among the two substrates, which differ only in a single methylene unit, as an opportunity which can allow us to gain deeper insights into the details of the I(III)-promoted reactions, whose mechanistic questions (Scheme 1) are far from settled. At this stage, we specifically asked do 3-fluoropiperidines form through 6-*endo*³⁷ or 5-*exo*/AIF/AIO mechanistic scenarios outlined in Scheme 1? If the latter is true, is the regioselectivity of the reaction then determined by the relative rates of AIF and RLC processes happening at the stage of the corresponding σ -alkyl-I^{III} species? What is the diastereodetermining step? What is the origin of chemoselectivity? In particular, we noted that 5-*exo* products are usually oxoaminated alkenes, which can be due to the C(*sp*³)-O reductive elimination process from I^{III}-center, while chemoselectivity (F/O) of 6-*endo* products can be expected to depend on the relative rates of AIO processes with F- and O-nucleophiles. We hope that answering these questions will enable us to provide the preparative guidelines for controlled synthesis of 3-fluoropiperidines using BF₃-activated I(III) reagents.

To answer the questions outlined above we conducted a comprehensive examination of BF₃-activated hypervalent iodine promoted fluorocyclizations on the **3a** and **3b** (Table 1). As mentioned before, the notation **a** and **b** have been used for substrates and corresponding products with the cyclopentyl (**a**) and cyclohexyl (**b**) substructure. Since, multiple products are formed, we classified them in Table 1 according to: a) the size of the newly formed ring, where **4** and **5** refer to 6-membered piperidine products while **6** and **7** refer to 5-membered pyrrolidine products, b) the stereochemistry of the newly formed stereocenter where the notion α (products **5** and **7**) and β (products **4** and **6**) inform about the relative stereochemical relationship among the β angular nitrile group and the functional group (**X** or CH₂**X**) at the formed stereocenter, and c) added group **X**, which can be either fluorine (F) or the corresponding carboxylate ligand (L = RCO₂). Lastly, we defined the relative involvement of aziridinium ion formation over reductive ligand coupling (AIF/RLC) as (**4-F+4-L**)/**6-L**.

Reacting alkenes **3a** and **3b** with **AR1** revealed that AIF is more favored over RLC in the **a**-system (AIF/RLC \sim 8.5:1) relative to the **b**-system (AIF/RLC \sim 1:1). Additionally, the AIF pathway is found to be suppressed by lowering the temperature (Table 1, entries 1-4). or by the addition of pyridine (Table 1, entry 5; conditions reported by Li³³). Importantly, the presence of pyridine also negatively impacts the chemoselectivity by giving a higher proportion of the acetoxyated products (**4b/5b/6b-OAc**). In contrast, we have discovered that by adding TBABF₄ to the reaction (Table 1, entries 6-7) the yield of 3-fluoropiperidines (**4a/5a-F** and **4b/5b-F**) can be greatly increased.

Next, switching the ligand on I(III) from acetate to pivalate shows a great increase in chemoselectivity favoring the aziridinium ion opening products (**4a/b-X** and **5a/b-X**) ($X = F, \text{OPiv}$), however, we still detect $\sim 34\%$ of the RLC-product (**6b-OPiv**) starting from **3b** (Table 1, Entry 8). This was the first evidence we collected that clearly demonstrates that the diastereoselectivity in such reactions is not solely substrate dependent but can be in fact tuned by altering the reagent structure. For instance, reagents with acetate and pivalate ligands (**AR1-2**) majorly produce compounds with β -stereochemistry, while the trichloroacetate-derived reagent (**AR4**, entries 11-12), as well as cyclic reagents (**CR1-2**, entries 13-15) favor pathways that yield products with α -stereochemistry. It is worth mentioning that no reaction was observed by mixing only **3b** and the I^{III} reagent in CH_2Cl_2 at room temperature after 48 h (Table 1, Entry 16), nor by combining only **3b** and $\text{BF}_3 \cdot \text{Et}_2\text{O}$ (Table 1, Entry 17). Thus, the reaction occurs only when both I^{III} and $\text{BF}_3 \cdot \text{Et}_2\text{O}$ are present (Table 1, Entries 1-15), which is in line with prior reports.³²

Table 1. Cyclization of **3a** and **3b** by I(III) reagents in the presence of $\text{BF}_3 \cdot \text{OEt}_2$

3a: n=0
3b: n=1
X = F or L

[(4-7)-F+(4-7)-L]=100%
AIF/RLC=[4-F+4-L]/6-L
 $\beta/\alpha = \frac{[(4,6)-F+(4,6)-L]}{[(5,7)-F+(5,7)-L]}$

PhilL₂

AR1: L=OAc
AR2: L=OPiv
AR3: L=ClCH₂CO₂
AR4: L=Cl₃CCO₂

CR1: L=OH
CR2: L=OAc

| Entry | S.m. ^a | Reagent | T (°C) | BF ₃ /BF ₄ ⁻ | Con. [%] ^b | F: 4:5:6:7 ^b | L: 4:5:6:7 ^b | AIF/RLC (β) | β/α ^d |
|-------|-------------------|------------------|--------|---|-----------------------|-------------------------|-------------------------|-------------|------------------|
| 1 | 3a | AR1 | 25 | 8/0 | >99 | a: 77 : 11 : 2 : 1 | a: 0 : 0 : 9 : 0 | 8.6 | 7.3 |
| 2 | 3a | AR1 | -78 | 8/0 | >99 | a: 82 : 4 : 0 : 0 | a: 0 : 0 : 13 : 1 | 6.3 | 19 |
| 3 | 3b | AR1 | 25 | 8/0 | >99 | b: 33 : 9 : 8 : 0 | b: 8 : 4 : 37 : 0 | 1.1 | 6.6 |
| 4 | 3b | AR1 | -78 | 8/0 | >99 | b: 26 : 2 : 6 : 0 | b: 15 : 4 : 47 : 0 | 0.87 | 16 |
| 5 | 3b | AR1 | 25 | 8/0/2 eq. Py | >99 | b: 22 : 3 : 1 : 0 | b: 18 : 9 : 47 : 0 | 0.85 | 7.3 |
| 6 | 3a | AR1 | 25 | 3/50 | >99 | a: 67 : 14 : 0 : 0 | a: 6 : 2 : 11 : 0 | 6.6 | 5.2 |
| 7 | 3b | AR1 | 25 | 3/50 | >99 | b: 39 : 12 : 6 : 0 | b: 6 : 6 : 28 : 2 | 1.6 | 3.9 |
| 8 | 3b | AR2 ^c | 25 | 3/0 | >96 | b: 37 : 15 : 7 : 0 | b: 0 : 3 : 29 : 0 | 1.3 | 4.1 |
| 9 | 3a | AR3 | 25 | 8/0 | >99 | a: 81 : 5 : 0 : 0 | a: 2 : 9 : 3 : 0 | >25 | 6.1 |
| 10 | 3b | AR3 | 25 | 8/0 | >99 | b: 27 : 13 : 3 : 0 | b: 9 : 15 : 27 : 6 | 1.3 | 1.9 |
| 11 | 3a | AR4 | 25 | 8/0 | >99 | a: 66 : 27 : 7 : 0 | a: 0 : 0 : 0 : 0 | >25 | 2.7 |
| 12 | 3b | AR4 | 25 | 8/0 | >99 | b: 20 : 42 : 3 : 0 | b: 9 : 20 : 6 : 0 | 4.8 | 0.61 |
| 13 | 3a | CR1 | 25 | 3/50 | >99 | a: 70 : 26 : 0 : 0 | a: 0 : 4 : 0 : 0 | >25 | 2.3 |
| 14 | 3b | CR1 | 25 | 3/50 | >99 | b: 20 : 56 : 0 : 0 | b: 0 : 6 : 9 : 0 | 2.2 | 0.47 |
| 15 | 3b | CR2 | 25 | 8/0 | >99 | b: 15 : 29 : 0 : 0 | b: 0 : 25 : 29 : 0 | 0.52 | 0.81 |
| 16 | 3b | AR1 | 25 | 0/0 | 0% | — | — | — | — |
| 17 | 3b or 3a | — | 25 | 8/0 | 0% | — | — | — | — |

^aReactions were carried in dry CH_2Cl_2 at ambient temperature with 1.2 equiv. of the corresponding I^{III} reagent; progress of the reactions was monitored by TLC (see SI for more details). ^bDetermined from gas chromatograms and/or ¹H NMR spectra of the neutral reaction mixtures. ^cSolution of the reagent in CH_2Cl_2 was added dropwise to a solution of **3b** and $\text{BF}_3 \cdot \text{OEt}_2$. ^dβ/α notion refers to the stereochemical relationship of X-group in piperidines or CH_2X group in pyrrolidines with respect to the β angular CN group, by analogy with steroidal systems.

Additionally, the plot of AIF/RLC ratio against the pK_a values for the corresponding ligand resulted in a linear correlation (Figure 5, plot). This is in agreement with our proposal that formation of five- and six-membered products is under Curtin-Hammett control⁴⁷ (Figure 5, Scheme), where *cis*- and *trans*-**11** interconvert via [1,3]-sigmatropic shift of iodine between two oxygens from the carboxylate.⁴⁵ Importantly, the finding (Figure 5, plot) that ratio $k_{\text{RLC}}/k_{\text{AIF}}$

can be influenced by the ligand acidity also implies that the RLC process can be envisioned as an internal attack of the oxygen on the electrophilic C(sp³) (Figure 5). Accordingly, more basic ligands show RLC rate enhancement since their oxygen atoms have greater nucleophilicity. This information can be of preparative relevance when trying to navigate the complex energy landscape of I(III) promoted reactions.

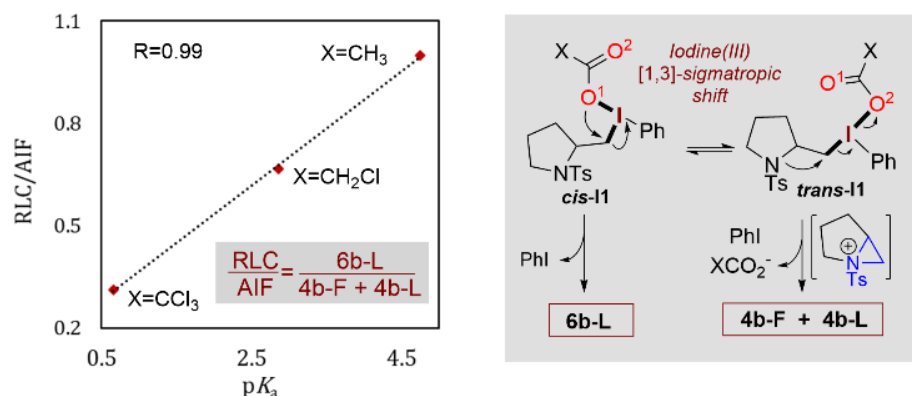
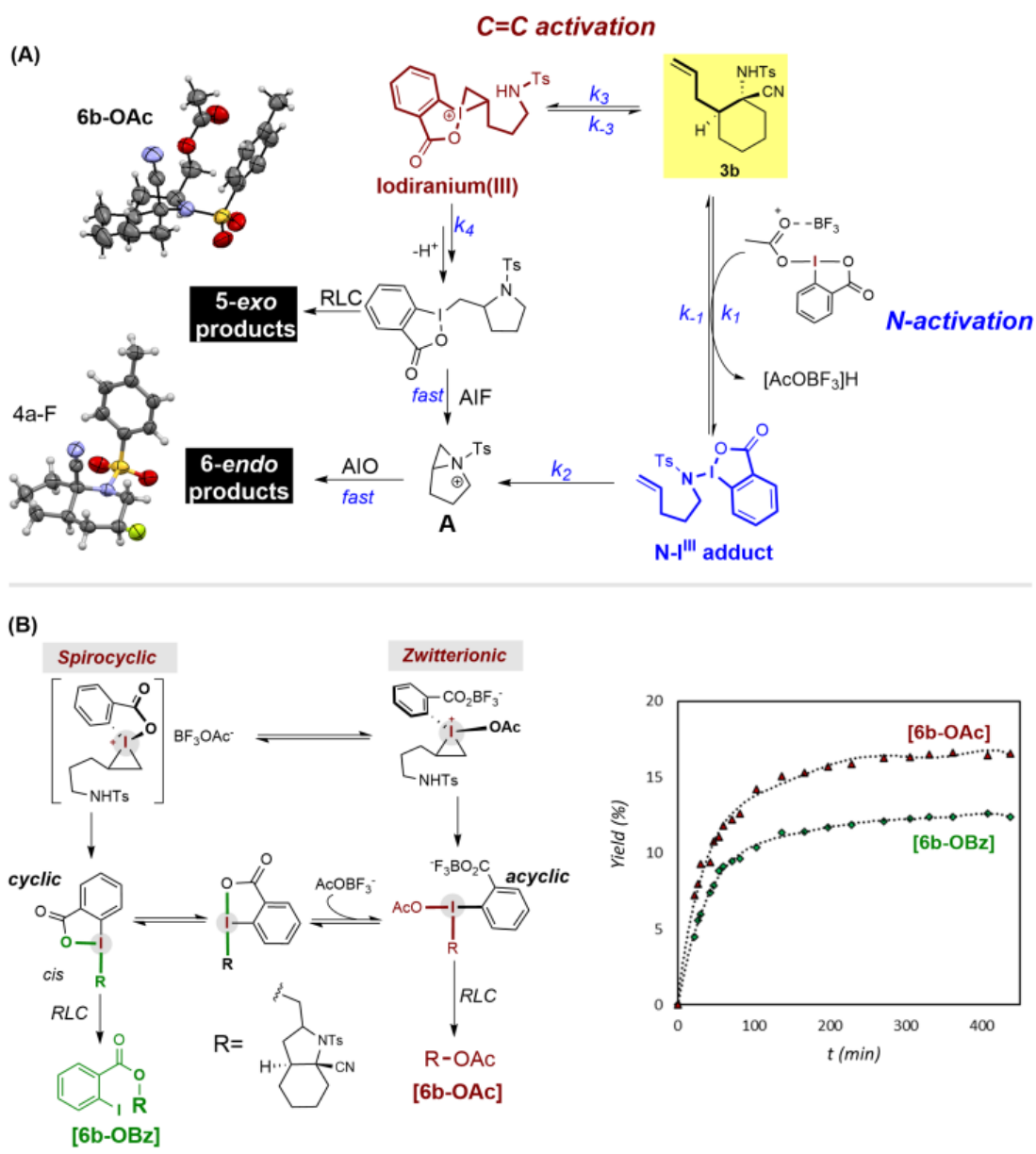


Figure 5. (Plot) Linear relationship between ligand's acidity (pK_a) and RLC/AIF ratio. (Scheme) Pathways leading to products of different ring size; structures have been simplified for clarity.

To gain further insight in the interplay among stereo-, regio-, and chemoselectivity we chose to monitor reactions with **3b** substrate and different classes of I(III) reagents via real-time (RT) multinuclear NMR spectroscopy. Interestingly, the reaction with acyclic reagent **AR1** was finished by the time the first spectrum was acquired (<5 min, Figure S43). On the contrary, the reaction with cyclic reagent **CR2** was significantly slower, allowing us to record {¹⁹F}¹H and {¹H, ¹³C}¹⁹F NMR spectra as a function of reaction time (Figure 6). Several important observations were made from these experiments.

The starting material (**3b**) directly converts to the corresponding products, with the proposed intermediates being NMR silent. The olefinic- and tosylamidic-proton resonances from **3b** steadily decayed away over time with parallel steady amplification of resonances that correspond to the products (**4b-F**, **5b-F**, **5b-L**, **6b-L**; L = **OAc** or **OBz** = 2-iodobenzoate). The formation of *N*-iodinated-**3b** was not observed. In case of an operative *N*-activation pathway (Scheme 2A, pathway b) it can be expected that the *N*-iodinated substrate would immediately transform into the products, so it doesn't form in a noticeable amount during the NMR experiment.³³ In other words, the outlined steady-state situation would involve the formation of the **N-I^{III}** adduct through AcO/TsN ligand exchange, which would have had to be the rate determining step (RDS = rate determining step, V = rate, V₁<V₂, Scheme 2A) to fit the observed spectral picture where there is no buildup of such an intermediate. Same can be expected if the equilibrium describing the formation of **N-I^{III}** adduct is significantly shifted towards the starting material (K₁<<1), even if this process is not the RDS.

Next, we found no NMR evidence of the iodiranium(III), which is the intermediate in the alternative C=C activation pathway (Scheme 1, pathway b). In case that such pathway operates, the observed absence of iodiranium(III) can be explained by either the formation of iodiranium(III) as the RDS (V₃<V₄) or cyclization as the RDS with a very unfavorable equilibrium for the formation of iodiranium(III) (V₃>V₄ with K₃<<1 preventing its ¹H NMR visibility; Scheme 2A). Anions BF₃OAc⁻ and BF₃OBz⁻ were detected in ¹⁹F and ¹¹B NMR spectra of the reaction (Figures 6 and S44). Crucially, this spectroscopic evidence additionally supports the hypothesis that BF₃L⁻ anions are fluoride transfer reagents.



Scheme 2. (A) The C=C and N-activation pathways, and X-ray structures of 5-*exo* (**6b-OAc**) and 6-*endo* (**4a-F**) products, the displacement ellipsoids are set at a 50% probability level; the structures of the intermediates are simplified for clarity. (B) The parallel formation of **6b-OAc** and **6b-OBz**, as measured from RT-NMR $\{^{19}\text{F}\}^1\text{H}$ NMR experiment (plot), led us to deduce that the reaction proceeds through iodiranium(III).

Time-dependent ^1H and ^{19}F NMR experiments (Figures S40-S44) revealed faster formation of BF_3OAc^- in comparison to BF_3OBz^- (Scheme 2B), with acetate methyl resonance from **CR2** moving downfield (c.a. 0.08 ppm) immediately after the addition of $\text{BF}_3 \cdot \text{Et}_2\text{O}$, and staying practically at the same chemical shift in all recorded time points (Figure 6). Considering this and the basicity of the two carbonyl oxygens ($\text{AcO}^- > \text{BzO}^-$), we propose that the asymmetric **CR2** reagent is majorly activated through BF_3 -coordination with the acetate ligand. Accordingly, we suggest that reaction of **CR2** with C=C bond is expected to yield spirocyclic iodiranium(III), which can be further opened to give zwitterionic iodiranium(III) (Scheme 2B). Next, the 5-*exo* cyclization followed by RLC or AIF/AIO (Scheme 2) results in the formation of the corresponding 5-*exo* (**6b-OAc** and **6b-OBz**) and 6-*endo* (**4b-F**, **5b-F**, **5b-OAc**, **5b-OBz**) (all observed in the RT-NMR experiments shown in Figure 6) products, respectively. In fact, our

initial hypothesis was that with cyclic reagents the RLC pathway will be suppressed due to reduced fluxionality of the carboxylate ligand on I^{III} once it is linked to the σ -aryl (cyclic σ -alkyl-I^{III} shown in Scheme 2B). Indeed, we observed the formation of **6b-OBz** (12%) in smaller quantities than **6b-OAc** (17%). The formation of **6b-OAc** can be explained by RLC from the acyclic I^{III} intermediate that can be formed through ligand metathesis reactions at the stage of iodonium(III)-ion and/or σ -alkyl-I^{III} (Scheme 2B). Overall, RT-NMR derived data strongly supports that a C=C activation pathway is operative, with the absence of the N-I^{III} adduct and the presence of 5-*exo* products (**6b-OAc** and **6b-OBz**) being crucial in ruling out the *N*-activation pathway. The unique structure and dynamics of iodonium(III)-ions generated from cyclic reagents are responsible for the significant modulation of diastereoselectivity (β/α), as well as the AIF/RLC ratio in the β -series (Table 1, entry 15). In addition, 3-fluoropiperidines were obtained in 45% yield with the ratio $F^{ax}/F^{eq} = 2:1$. Interestingly, our findings contrast the mechanistic proposal for ArIF₂-mediated fluorocyclizations, where it was reported that reaction begins via *N*-activation.³⁵

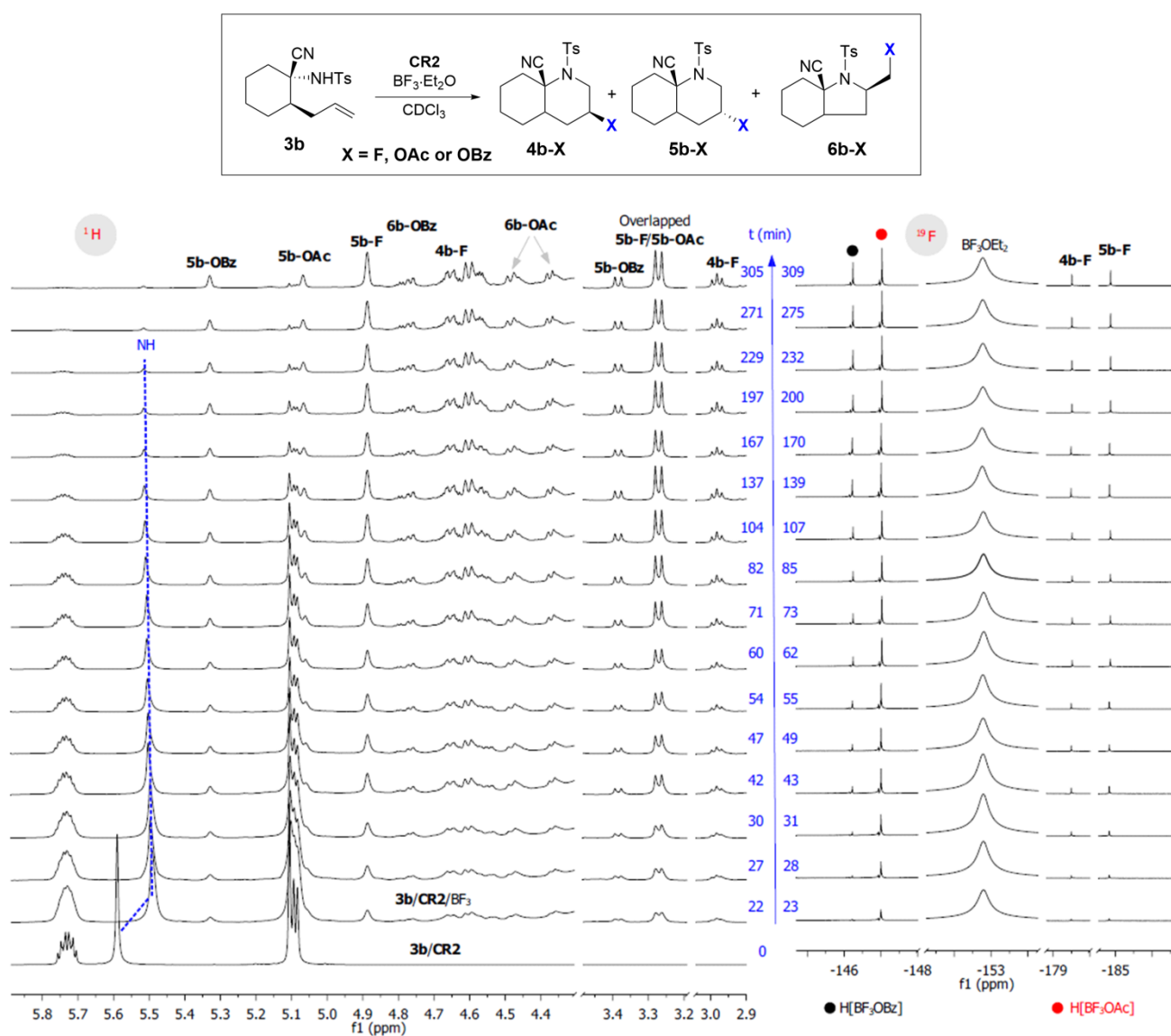
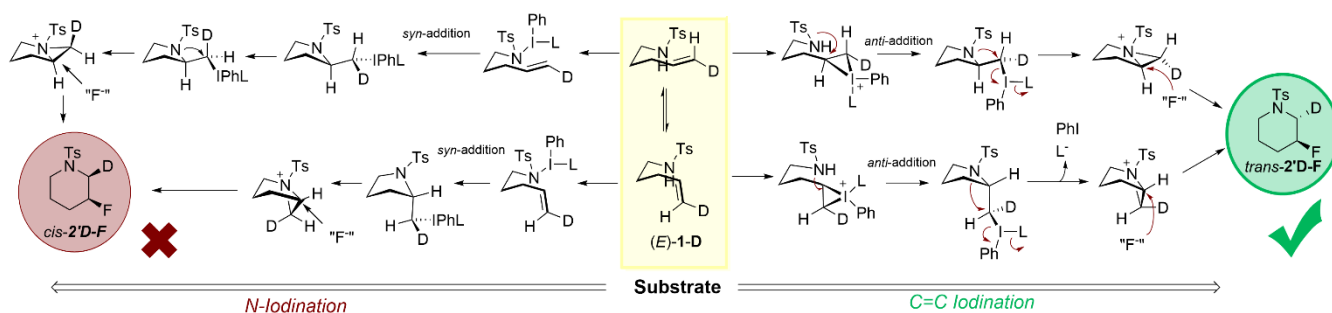


Figure 6. The reaction of **3b** with **CR2**/**BF₃**, followed by $\{^{19}\text{F}\}^1\text{H}$ (800 MHz) and $\{^1\text{H},^{13}\text{C}\}^{19}\text{F}$ NMR (752 MHz) in CDCl_3 at 298 K (see Figure S44 for details).

Using our comparative analysis approach on **3a/b** substrates (Table 1) we have found that the reactions with two acyclic reagents bearing pivalate (**AR2**) and trichloroacetate (**AR4**) groups show significantly different diastereoselectivities. However, the reactions with **AR2** and **AR4** are much faster relative to cyclic reagents, which has prohibited their detailed inspection using the multinuclear RT NMR approach. In anticipation to probe the mechanistic questions with acyclic reagents bearing rather simple ligands that give starkly different stereochemical outcomes, we conducted the reactions with deuterium incorporated substrate (*E*)-**1-D**. Our stereochemical analysis suggests that C=C iodination pathway would furnish *trans*-**2'D-F**, while *N*-iodination pathway would yield *cis*-**2'D-F** (Scheme 3). Importantly, we found that *trans*-**2'D-F** is being exclusively formed in both reactions. This strongly suggests that the C=C activation pathway is operative also with acyclic reagents **AR2** and **AR4**, which aligns with the mechanistic proposal derived using multinuclear RT NMR approach on cyclic reagents.



Scheme 3. Intramolecular aminofluorinations of (*E*)-**1-D** substrate by means of two different PhIL₂ reagents, **AR2** (L = Me₃CCO₂⁻) and **AR4** (L = Cl₃CCO₂⁻), give exclusively *trans*-**2'D-F**, which speaks in favor of C=C activation pathway.

¹H NMR has shown that BF₃ induces the reduction of σ-aryl-I^{III} reagents to the corresponding aryl iodides. For example, **AR1** (so called PIDA) can produce PhI (Figure S40). At this stage, we presupposed that **AR1-4** could transfer their ligands to σ-alkyl-I^I ⁴⁸ and saw this as an opportunity to further deconvolute stereo-, regio- and chemoselectivity of the reaction by evaluating the reactivity of *in situ* generated σ-alkyl I^{III} compounds [R'-I(RCO₂)₂]. Combining 2-iodomethylpyrrolidines with acyclic I^{III} reagents and BF₃ resulted in the immediate formation of 3-fluorinated and 3-oxygenated piperidines (Figure 7A-C), but also carboxyloxymethyl pyrrolidines in some cases. In contrast, no reaction was observed with **CR2**/BF₃ (Figure 7D). Importantly, by working on stereodefined **6a/b-I** and **7b-I** we have discovered that ring enlargement reactions are stereospecific. Furthermore, σ-alkyl-Br^I and σ-alkyl-Se^{II} were inert even towards acyclic reagents under studied conditions. This is likely due to more difficult oxidative addition on less electron rich Br^I and Se^{II} centers. Such findings can be highly useful in performing chemoselective and stereospecific transformations on molecules with complex chemical structures that carry numerous functionalities.

At this stage, by taking into account the results of cyclization and rearrangement reactions we have drawn several mechanistic conclusions. First, in the reactions of I^{III}/BF₃ with alkenes, the cyclization is the diastereodetermining step since σ-alkyl I^{III} rearrange stereospecifically (Figures 7B-C and S51-59). Second,

final 5-*exo* products (**2-L** and **6b-L**) are formed via the RLC pathway in both cyclization and ring enlargement reactions. Third, the RLC pathway is more favored in cyclizations than in rearrangements (RLC/AIF: **11**>**12** – especially for more basic ligands), most likely due to the presence of stronger *trans*-influencing ligand (Ph) in *cis*-**11**, in comparison to *cis*-**12** (RCO₂).^{49,50} Finally, basic and bulky carboxylate ligands (*i.e.* PivO⁻) increase the F/O ratio of piperidine products by suppressing RLC and favoring the AIF pathway, and that the structure of the substrate influences the RLC/AIF ratio.

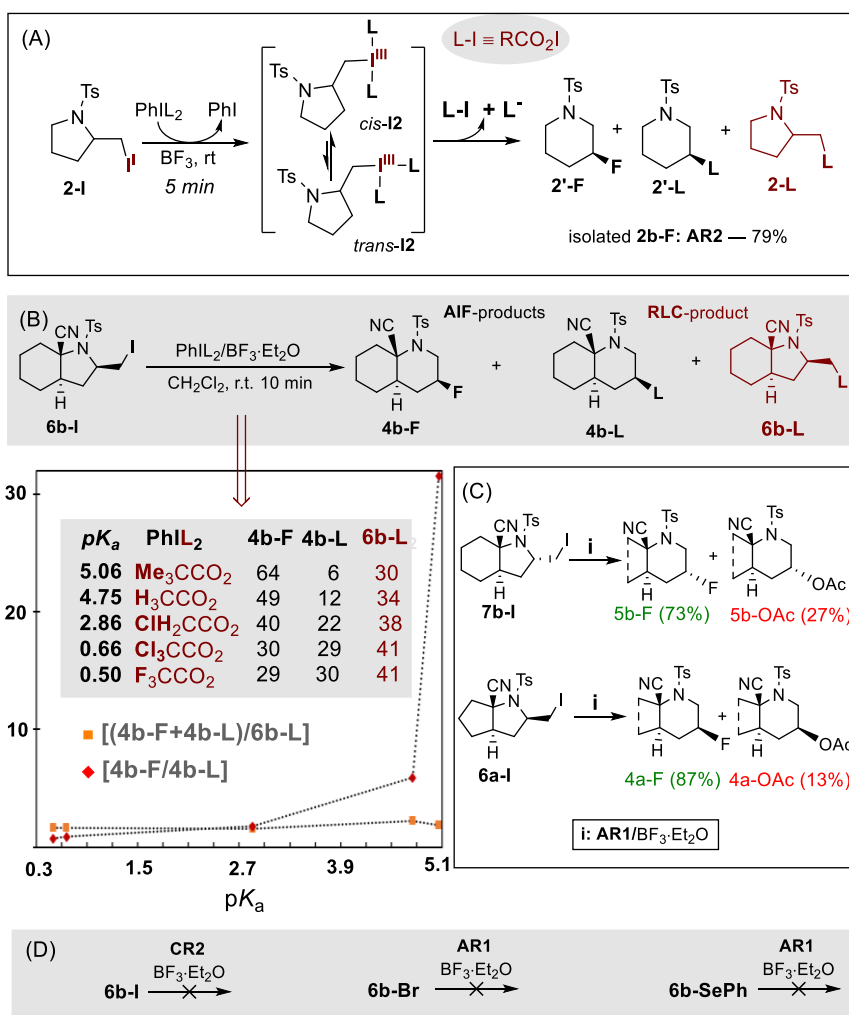


Figure 7. Reactivity of σ -alkyl-I^{III} species generated through oxidative ligand transfer reaction from ArI^{III}-dicarboxylates and substrates: (A) **2-I**; (B) **6b-I**, the product distribution depends on the nature of the ligand (L) as shown in the plot; (C) **7b-I** and **6a-I** (D) **6b-I** doesn't react with **CR2**; σ -alkyl-Br^I and σ -alkyl-Se^{II} are unreactive with **AR1**.

Regioselectivity. As mentioned above, the dissimilar reactivity of alkenes **3a** and **3b** in traditional cyclizations (Figures 4 and S17-18) arise from the difference in strain that is being developed in the corresponding 5-*exo*-TS[‡] (**3a**>**3b**). We assumed that iodiranium(III) is more electrophilic than traditional

iodiranium(I) ($C=C + I_2$). Accordingly, the early TS^\ddagger was predicted for ring closure via I^{III} -iraniums, enabling efficient 5-exo cyclization in both systems. The destiny of the σ -alkyl- I^{III} intermediates dictates the final product ring size. In other words, AIF must outcompete RLC for the reaction to show high regioselectivity for six-membered products. Given our experiments outlined in Table 1 (entries 1 and 3), we expected that the extra methylene in **b** with respect to **a** would cause a significant difference in AIF/RLC ratios in the two systems. This is also found in the rearrangement experiments where σ -alkyl- I^{III} compounds generated from **6a-I** undergo exclusively AIF while those generated from **6b-I** give considerable amount of the RLC product (**6b-OAc**; Figure 7). To rationalize the substrate influence on the AIF/RLC ratio we propose that $k_{RLC}(\mathbf{a}) \sim k_{RLC}(\mathbf{b})$ while $k_{AIF}(\mathbf{a}) \gg k_{AIF}(\mathbf{b})$, which should hold true considering that the RLC pathway does not involve the steric interaction of the exocyclic CH_2X group with the bicyclic moiety, while it does in the case of AIF processes. Thus, the factors determining the energy difference between σ -alkyl- I^{III} intermediate and the TS^\ddagger for AIF (ΔG^\ddagger_{AIF}) should reveal the origin of the dissimilar reactivity between **a** and **b**. Unfortunately, low persistence of σ -alkyl- I^{III} species forbid direct experimental studies of the conformational preference in **6a- I^{III}** and **6b- I^{III}** . Therefore, we performed conformational analysis in solution (room temperature 1H , ^{13}C , ^{15}N NMR) and solid state (single crystal X-ray) on **6a-X** and **6b-X** systems ($X = H, OAc, SePh, Cl, Br, I$), where the σ -accepting ability⁴⁹ (energy of σ^*_{C-X}) and degree of polarization of $C-X$ bonds were systematically varied. Our approach involved solution NMR conformational analysis that helped judge the relative strength of the important stereoelectronic interactions (see SI for details). Since $n_N \rightarrow \sigma^*_{C-I(III)}$ represents the $N-CH_2$ bond forming event, we hypothesized that this orbital interaction should be responsible for the stabilization of *antiperiplanar* (*ap*) arrangement between TsN and X , with an α -positioned tosyl group (Figure 8A). Indeed, this conformation was found to be prevalent in solution for all **6a** and **6b** systems bearing halogens ($X = Cl, Br, I$), while *+sinclinal* (*+sc*) conformation was detected in the case of $X = OAc$ (Figures S60-61 and Table S5). Importantly, a linear relationship was found by plotting $\Delta\delta(^{13}CH_2X)$ against $C-X$ bond distances ($X = H, Cl, Br, I$; Figure 8C), which agrees with expected trend that anomeric (*i.e.* $\sigma(C-N) \rightarrow \sigma^*_{C-X}$) and homoanomeric ($n_N \rightarrow \sigma^*_{C-X}$) interactions are the strongest for σ^*_{C-X} with the lowest energy/longest $C-X$ bond in the series.

Next, conformational analysis in the solid state was performed by inspecting X-ray diffraction derived crystal structures of **6a-Br** and **6b-Br** where we noticed that the $N-C-C-Br$ fragments are in *ap*-conformation in both cases. After measuring the $N-C-C-Br$ torsion angles, as well as the length of the $C-Br$ bonds for these two compounds, we noticed that the **6a-Br** system has an almost perfect 180° torsion angle and a somewhat longer $C-Br$ bond than **6b-Br**. Therefore, we propose that hyperconjugative interactions with σ^*_{C-X} are stronger in **6a- I^{III}** than in **6b- I^{III}** systems as a result of strain-induced HOMO-raising effect.⁵⁴ On the other hand, homologation of **6a** into **6b** has steric consequences. During the formation of the $C-N$ bond, the CH_2X -hydrogen and Ts -group are being pushed towards the bicyclic moiety, which presumably increases steric compression among the *axial* substituents (Figure 8D) on β - and α -sides. To sum up, we propose that synergy of weaker donation into $\sigma^*_{C-I(III)}$ and stronger steric repulsions in the AIF TS^\ddagger are responsible for the higher propensity of the **6b** system to undergo RLC in comparison to **6a** (Figure 8E).

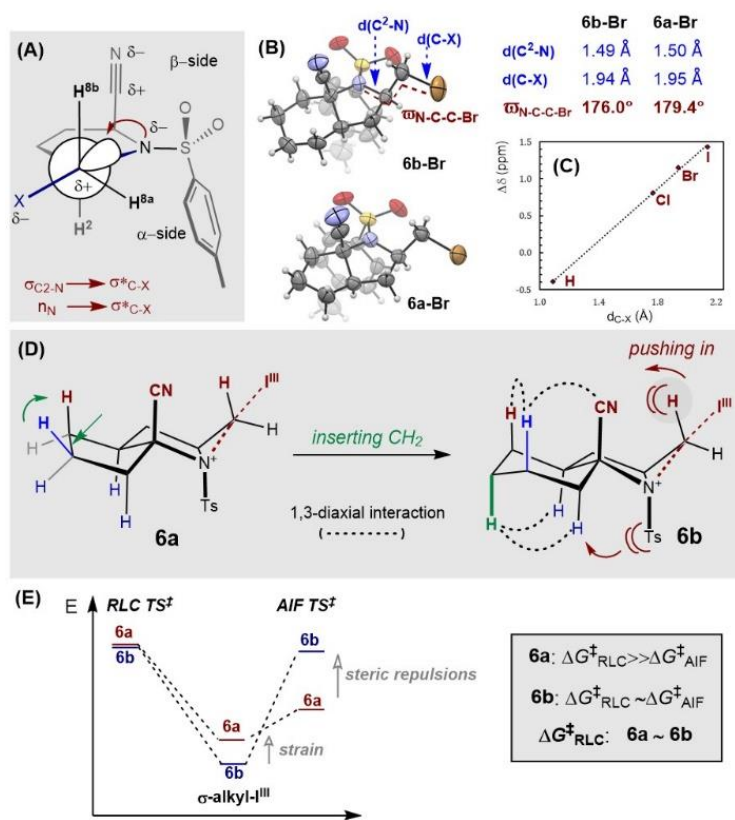


Figure 8. (A) Important interactions in α -TsN/X-ep conformation; (B) X-ray structures and important structural parameters found for **6a-Br** and **6b-Br**, the displacement ellipsoids are set at a 50% probability level. (C) Linear relationship between the length of C—X bond (d_{C-X}) and $\Delta\delta(^{13}\text{CH}_2\text{X}) = \delta(\text{6b-X}) - \delta(\text{6a-X})$. (D) Steric effects in AIF transition states. (E) Qualitative energy diagram of σ -alkyl-I^{III} species **6a-I^{III}** and **6b-I^{III}** and the corresponding RLC and AIF transition states.

Diastereoselectivity. As mentioned earlier, the choice of the reagent affects the diastereoselectivity of aminofluorination of alkenes **3a-b**, with the magnitude of the modulation being substrate dependent (Table 1). Four diastereomeric iodiranium(III) ions (Figure 9A) could be formed in the reaction of a prochiral alkene and I^{III} reagent. Steric effects related to the substrate favor the *Si*-approach, due to destabilizing Prelog transannular strain in the TS^\ddagger for 5-*exo* cyclization going through iodonium ions formed via *Re*-approach (Figure 9B). However, the *Re*-approach can be favored by using reagents that bear ligand(s) with moieties capable of interacting with positively polarized hydrogens (Figure 9C). The effect of the transannular strain can be reduced through the stabilization of the TS^\ddagger *Re-3b-1* and *Re-3b-2* (Figure 9C) via attractive non-covalent interactions, facilitating the formation of *axial*-fluoride products. Aside of explicit electrostatic interactions which are proposed in the case of cyclic reagents **CR1-2**, weak but cooperative multivalent C—H \cdots Cl—C hydrogen bonds⁵⁵⁻⁵⁷ are being harnessed in the case **AR4**. Therefore, we propose that the net diastereoselectivity (β/α) is determined in the cyclization step by $\Delta G^\ddagger_{\text{Re-5-exo}}/\Delta G^\ddagger_{\text{Si-5-exo}}$, which is under the influence of steric and electrostatic interactions along the reaction coordinate. Namely, we rationalized that **AR1-2** (L = OAc and OPiv) promote pyrrolidine ring formation through *Si-3b-1* and *Si-3b-2*, while **CR1-2**

and **AR4** ($L = \text{CCl}_3\text{CO}_2^-$) more prominently promote the cyclization through I^{III} -iranium originated from *Re*-attack of I^{III} on the $\text{C}=\text{C}$ bond (*Re-3b-1* and *Re-3b-2*, Figure 9A).

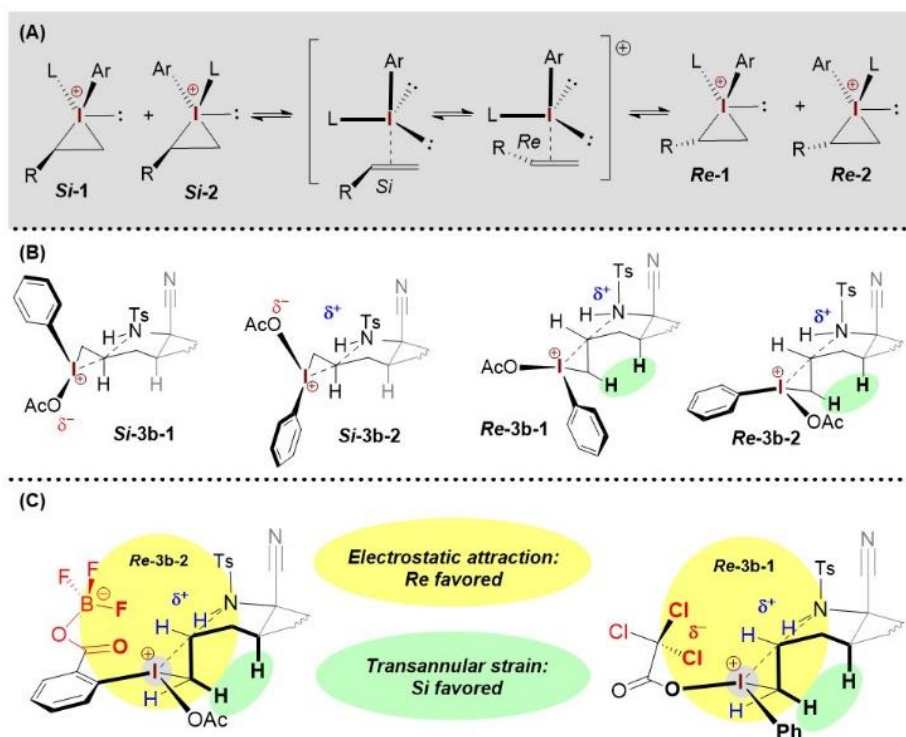


Figure 9. (A) Four diastereomeric iodiranium(III) ions; (B) The transition states for 5-exo ring closures from the corresponding iodiranium(III) ions; (C) Non-covalent interactions influencing the energy of the 5-exo TS^\ddagger .

Chemoselectivity. The described cyclization experiments suggest that the chemoselectivity in six-membered products is determined by the nature and the concentration of the corresponding F- and O-nucleophiles. Specifically, the highest **2'-F/2'-O** ratio in cyclization reactions is obtained with the reagents having carboxylates which are more basic but less nucleophilic, such as pivalate (Figure 10). This is in agreement with the proposal that free carboxylates open the aziridinium ion to give oxygenated products, hence with more basic ligands there is a higher concentration of $[\text{RCO}_2\text{BF}_3]^-$ present in the solution, favoring the formation of **2'-F**. In addition, increased steric bulkiness decreases the nucleophilicity of the free carboxylate, so the present concentrations (Figure 10, eq. 1) are insufficient in promoting effective aminoxygenation. Our experiments strongly suggest that the nucleophilic fluoride species that open the aziridinium ion are $\text{RCO}_2\text{BF}_3^-$, while the actual O-nucleophile is the free carboxylate (Figure 10).

Interestingly, the corresponding **2'-F/2'-O** ratios measured for ring-enlargement reactions (Figures 10 and S45-50) are higher for all examined ligands Ar when compared to ratios obtained in the corresponding cyclization reactions. To rationalize this finding, we note that 2 equiv. of the carboxylate are released during cyclization. However, in the ring enlargement reactions the σ -alkyl- I^{III} species release 1 equiv. of carboxyl

hypiodate (RCO_2I) and 1 equiv. of the carboxylate. These two can then react according to eq. 2 shown in Figure 10.⁵⁸ This extra equilibrium explains the difference in chemoselectivity between cyclization and ring expansion, where free carboxylate that delivers oxygenated **2'-O** product is not only mitigated through the reaction with BF_3 (Figure 10, eq. 1) but also the reaction with RCO_2I (Figure 10, eq. 2). Importantly, the equilibrium showcased in eq. 1 within Figure 10 provides a clear explanation of why dropwise addition, discussed above, of the I^{III} -dicarboxylate solution to the mixture of the substrate and $\text{BF}_3 \cdot \text{Et}_2\text{O}$ provides two-fold higher yields of fluorinated products as compared to adding the $\text{BF}_3 \cdot \text{OEt}_2$ to the solution of the substrate and the corresponding aryl iodine(III) reagent (see Table in Figure 3, entry 1 and 2), which is of preparative relevance.

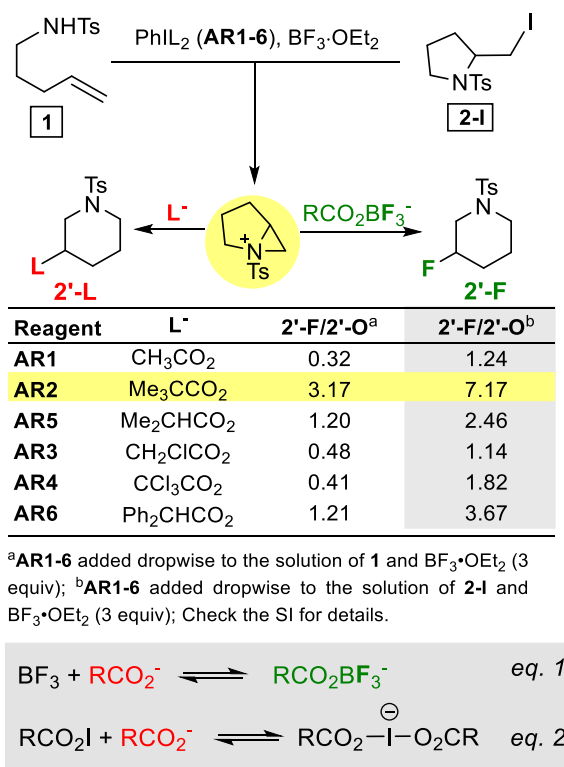


Figure 10. Comparison of chemoselectivity during piperidine product formation via cyclization of **1** (Table S1) and ring expansion of **2-I** (Table S2), with the important equilibria that affect the outcome.

Preparative relevance. Finally, the synthetic significance of simple aryl iodine(III)carboxylates such as **AR2**, **CR1** and **AR4** in the synthesis of diastereomeric 3-fluoropiperidines is shown in Figure 11. First, we found that generally the selectivity for fluorinated over oxygenated products can be increased by dropwise addition of a CH_2Cl_2 solution of the corresponding iodine(III) reagent into the mixture of substrate and $\text{BF}_3 \cdot \text{Et}_2\text{O}/\text{TBABF}_4$ (Figure 11A). For substrates with a high preference for the AIF pathway (i.e. **3a**), it is enough to use **AR2** and $\text{BF}_3 \cdot \text{Et}_2\text{O}$ to reach good yields of the fluorinated products (conditions A in Figure 11), while the addition of TBABF_4 increases the yield of 3-fluoropiperidines by promoting AIF pathway in the case of substrates with higher propensity for RLC pathway (i.e. **3b**, conditions D, Figure 11). Importantly,

the diastereoselectivity of the reaction depends on the Ar^{III}-dicarboxylate reagent used. Specifically, acyclic iodine(III) reagents with the pivalate (**AR2**, conditions A in Figure 11) and trichloroacetate (**AR4**) ligands cause significantly different outcomes in the diastereoselectivity of the transformation. Interestingly, the cyclic reagent **CR1** shows analogous behavior to **AR4** (PhI(CCl₃CO₂)₂) in terms of diastereoselectivity, though, the acyclic reagent requires significantly shorter reaction times. Accordingly, larger quantities of 3-fluoropiperidine that was the minor stereoisomer in the reaction with **AR2** can be obtained by reacting the corresponding alkenyl tosylamide with **AR4** or **CR1** reagents. For example, **8** gives *trans*-**12** (55%) as a major product with **AR2**, while *cis*-**12** (60%) was the principal product in the reaction with **CR1**. Also, complete switch in the distereoselectivity is observed in the cyclization of **3b** with different reagents, where **AR2** favors **5b-F** (64%), while **4b-F** (53-60%) is favored by **CR1** or **AR4**. In the case of substrates **9**, **10**, and **3a** the diastereoselectivity was not as dramatically modulated by using different reagents as it was with **8** and **3b** substrates. However, it was still prominent enough to allow the isolation of both diastereomeric fluorides in appreciable yields. In this light, *cis*-**13** was obtained in 62% yield from **9** using **AR2**, while *trans*-**13** was isolated in 34% yield with **AR4** as a reagent. Similarly, *cis*-**14** (35%) was the major product in the reaction of **10** with **AR2**, while *trans*-**14** (63%) dominated in the reaction with **AR4**. Lastly, the substrate **11**, bearing two methyl groups in the allylic position, showed the same stereochemical outcome under different reaction conditions. One of the possible explanation for this intriguing observation might be that the steric crowding around the C=C bond has promoted the *N*-iodination pathway. However, at this moment there is no experimental evidence to corroborate this hypothesis.

| Substrate | | | | | | |
|--------------------|---------------------------------------|--------------------------------------|--------------------------------------|--------------------------------------|---------------------------------------|--|
| Products | | | | | | |
| <i>dr</i> (NMR) | A: 29 : 71 B: 90 : 10 C: 94 : 6 | A: 84 : 16 B: — : — C: 59 : 41 | A: 46 : 54 B: — : — C: 12 : 88 | A: > 99 : 1 B: — : — C: — : 63 | A: 5 : 95 B: 27 : 73 C: 28 : 72 | A: 30 : 70 B: 72 : 28 C: 67 : 33 |
| Isolated yield (%) | A: — : 55 B: 60 : — C: — : — | A: 62 : — B: — : — C: 45 : 34 | A: 35 : 32 B: — : — C: 4 : 63 | A: — : 65 B: — : — C: — : 63 | A: 3 : 80 B: 25 : 70 C: 26 : 65 | D: 20 : 64 B: 53 : 20 C: 60 : 22 |

A: 1.2 equiv. **AR2**, 5.0 equiv. BF₃·Et₂O; B: 1.2 equiv. **CR1**, 5.0 equiv. BF₃·Et₂O, 30.0 equiv. TBABF₄; C: 1.2 equiv. **AR4**, 5.0 equiv. BF₃·Et₂O, 30.0 equiv. TBABF₄;
D: 1.2 equiv. **AR2**, 5.0 equiv. BF₃·Et₂O, 30.0 equiv. TBABF₄.

Figure 11. Synthesis of diastereomeric 3-fluoropiperidines through intramolecular aminofluorination of alkenyl tosylamides using aryliodine(III) dicarboxylates and Et₂O·BF₃. The products are drawn in the conformations found by solution NMR spectroscopy.

Conclusion

In summary, we have experimentally inspected the mechanism of I^{III}-dicarboxylate/BF₃ promoted intramolecular aminofluorinations of unactivated olefins and discussed the origins of selectivity of this transformation in detail. The main challenge of the reaction is overcoming competitive oxoamination, which can originate from reductive ligand coupling (RLC) at the stage of σ -alkyl-I^{III} intermediate and/or preferential aziridinium ion opening with O-nucleophiles (RCO₂⁻). We have provided guidelines on how to troubleshoot these reactions depending on which mechanistic step influences chemo- and diastereoselectivity.

Experimental results indicate that the aforementioned reactions proceed through a C=C iodination pathway. In addition, the diastereoselectivity is determined at the stage of 5-*exo* cyclization and it is influenced by steric and electronic effects operating within iodonium(III) ion(s) and the corresponding transition state for pyrrolidine ring formation. Importantly, it is possible to alter the ratio of *axial*- and *eq*-C—F products by the proper choice of reagent. The regioselectivity (ring size) is dictated by the propensity of the σ -alkyl-I^{III} intermediate to undergo AIF and RLC processes, which is dictated by steric and stereoelectronic effects within the substrate, but it can be manipulated by the nature of the ligands on I^{III}, as well as electric field modulation by the addition of electrolytes (TBABF₄). Finally, chemoselectivity in six-membered products is determined by relative rates of aziridinium ion opening by F- and O-nucleophiles (RCO₂BF₃⁻ vs. RCO₂⁻, respectively). We have shown that basic, non-nucleophilic carboxylates (PivO⁻) are optimal for highly chemoselective aziridinium ion opening to provide 3-fluoropiperidines. By revealing the influence of different parameters on the outcome of the reaction, the stage is now set for a more predictable usage of easily accessible and stable aryl iodine(III) dicarboxylates in operationally simple syntheses of fluorinated azaheterocycles. These findings are relevant for medicinal chemistry, among other areas, where preparation of diastereomeric fluorinated piperidines is highly desirable.^{13,14}

Experimental Section

All experimental procedures, characterization data, original spectra, etc. are provided in the Supporting Information.

ASSOCIATED CONTENT

Data Availability Statement

The data underlying this study are available in the published article and its Supporting Information.

Supporting Information Statement

Supporting Information 1: Experimental procedures for the synthesis of all substrates and reagents, reaction of iodocyclization and aminofluorination, and crystallographic data (PDF); Supporting Information 2: NMR and mass spectra for all compounds (PDF). The Supporting Information files are available free of charge on the ACS Publications website.

Crystallographic data

Deposition numbers 2239681 (for **3a**), 2239682 (for **3b**), 2239683 (for **4a-F**), 2239684 (for **6a-Br**), 2239685 (for **6a-I**), 2239686 (for **6b-OAc**), 2239687 (for **6b-I**), and 2239688 (for **6b-Br**) contain the supplementary crystallographic data for this paper. These data are provided free of charge by the Cambridge Crystallographic Data Centre.

AUTHOR INFORMATION

*Corresponding Authors

Dr. B.M. Šmit, E-mail: biljana.smit@uni.kg.ac.rs

Dr. R.Z. Pavlović, Current address: Simpson Querrey Institute for BioNanotechnology, Northwestern University, Chicago, Illinois 60611, United States, E-mail: radoslav.pavlovic@northwestern.edu

Aithors contribution

‡These authors have contributed equally. Previous address: University of Belgrade, Faculty of Chemistry, Studentski trg 16, 11000 Belgrade, Serbia

†Current address: Johns Hopkins University, Department of Chemistry, 3400 North Charles St, Baltimore, MD21218, United States

NOTES

The authors declare no competing financial interest

ACKNOWLEDGEMENT

This work was financially supported by the Ministry of Science, Technological Development and Innovations of the Republic of Serbia (Grant numbers 451-03-47/2023-01/200026, 451-03-47/2023-01/200168, 451-03-47/2023-01/200125 and 451-03-47/2023-01/200378). The authors are highly grateful to Prof. Dragana R. Milić from University of Belgrade, Faculty of Chemistry and Prof. Jovica D. Badjić from The Ohio State University for supporting us and giving us space to perform parts of this research. The authors appreciate accommodations provided by Prof. Vladimir Savić from University of Belgrade, Faculty of Pharmacy to measure some of the ¹⁹F NMR spectra with the assistance of Dr. Zoran Miladinović from The Institute of General and Physical Chemistry Belgrade. This study made use of the Campus Chemical Instrument Center NMR facility at The Ohio State University and hereby the authors are thankful to Dr. Tanya Whitmer and Dr. Alexandar L. Hansen for their assistance with some of the NMR data acquisition.

REFERENCES

- (1) B. M. Trost, Selectivity: A Key to Synthetic Efficiency, *Science* **1983**, 219, 245.
- (2) P. A. Wender, B. L. Miller, Synthesis at the Molecular Frontier, *Nature* **2009**, 460, 197.
- (3) R. A. Shenvi, D. P. O'Malley, P. S. Baran, Chemoselectivity: The Mother of Invention in Total Synthesis, *Acc. Chem. Res.* **2009**, 42, 530.
- (4) B. L. W. Hernandez, D. Sarlah, Empowering Synthesis of Complex Natural Products *Chem. Eur. J.* **2019**, 25, 13248.
- (5) D. C. Blakemore, L. Castro, I. Churcher, D. C. Rees, A. W. Thomas, D. M. Wilson, A. Wood, Organic Synthesis Provides Opportunities to Transform Drug Discovery, *Nat. Chem.* **2018**, 10, 383.
- (6) K. R. Campos, P. J. Coleman, J. C. Alvarez, S. D. Dreher, R. M. Garbaccio, N. K. Terrett, R. D. Tillyer, M. D. Truppo, E. R. Parmee, The Importance of Synthetic Chemistry in the Pharmaceutical Industry, *Science* **2019**, 363, 6424.

(7) A. Aspuru-Guzik, M. H. Baik, S. Balasubramanian, R. Banerjee, S. Bart, N. Borduas-Dedekind, S. Chang, P. Chen, C. Corminboeuf, F. X. Coudert, L. Cronin, C. Crudden, T. Cuk, A. G. Doyle, C. Fan, X. Feng, D. Freedman, S. Furukawa, S. Ghosh, F. Glorius, M. Jeffries-El, N. Katsonis, A. Li, S. Snogerup Linse, S. Marchesan, N. Maulide, A. Milo, A. R. H. Narayan, P. Naumov, C. Nevado, T. Nyokong, R. Palacin, M. Reid, C. Robinson, G. Robinson, R. Sarpong, C. Schindler, G. S. Schlau-Cohen, T. W. Schmidt, R. Sessoli, Y. Shao-Horn, H. Sleiman, J. Sutherland, A. Taylor, A. Tezcan, M. Tortosa, A. Walsh, A. J. B. Watson, B. M. Weckhuysen, E. Weiss, D. Wilson, V. W. W. Yam, X. Yang, J. Y. Ying, T. Yoon, S. L. You, A. J. G. Zarbin, H. Zhang, Charting a Course for Chemistry, *Nat. Chem.* **2019**, *11*, 286.

(8) T. M. Trnka, R. H. Grubbs, The Development of L2X2Ru=CHR Olefin Metathesis Catalysts: An Organometallic Success Story, *Acc. Chem. Res.* **2001**, *34*, 18.

(9) D. O'Hagan, Pyrrole, Pyrrolidine, Pyridine, Piperidine and Tropane Alkaloids, *Nat. Prod. Rep.* **2000**, *17*, 435.

(10) S. Nara, R. Tanaka, J. Eishima, M. Hara, Y. Takahashi, S. Otaki, R. J. Foglesong, P. F. Hughes, S. Turkington, Y. Kanda, Discovery and Structure-Activity Relationships of Novel Piperidine Inhibitors of Farnesyltransferase, *J. Med. Chem.* **2003**, *46*, 2467.

(11) Z. Pei, X. Li, T. W. von Geldern, K. Longenecker, D. Pireh, K. D. Stewart, B. J. Backes, C. Lai, T. H. Lubben, S. J. Ballaron, D. W. A. Beno, A. J. Kempf-Grote, H. L. Sham, J. M. Trevillyan, Discovery and Structure-Activity Relationships of Piperidinone- and Piperidine-Constrained Phenethylamines as Novel, Potent, and Selective Dipeptidyl Peptidase IV Inhibitors, *J. Med. Chem.* **2007**, *50*, 1983.

(12) E. Vitaku, D. T. Smith, J. T. Njardarson, Analysis of the Structural Diversity, Substitution Patterns, and Frequency of Nitrogen Heterocycles among U.S. FDA Approved Pharmaceuticals, *J. Med. Chem.* **2014**, *57*, 10257.

(13) E. P. Gillis, K. J. Eastman, M. D. Hill, D. J. Donnelly, N. A. Meanwell, Applications of Fluorine in Medicinal Chemistry, *J. Med. Chem.* **2015**, *58*, 8315.

(14) J. Wang, M. Sánchez-Roselló, J. L. Aceña, C. Del Pozo, A. E. Sorochinsky, S. Fustero, V. A. Soloshonok, H. Liu, Fluorine in Pharmaceutical Industry: Fluorine-Containing Drugs Introduced to the Market in the Last Decade (2001-2011), *Chem. Rev.* **2014**, *114*, 2432.

(15) K. Müller, C. Faeh, F. Diederich, Fluorine in Pharmaceuticals: Looking Beyond Intuition, *Science* **2007**, *317*, 5846, 1881.

(16) M. Aufiero, R. Gilmour, Informing Molecular Design by Stereoelectronic Theory: The Fluorine Gauche Effect in Catalysis, *Acc. Chem. Res.* **2018**, *51*, 1701.

(17) D. Cahard, V. Bizet, The Influence of Fluorine in Asymmetric Catalysis, *Chem. Soc. Rev.* **2014**, *43*, 135.

(18) D. O'Hagan, Understanding Organofluorine Chemistry. An Introduction to the C-F Bond, *Chem. Soc. Rev.* **2008**, *37*, 308.

(19) N. A. Meanwell, Fluorine and Fluorinated Motifs in the Design and Application of Bioisosteres for Drug Design, *J. Med. Chem.* **2018**, *61*, 5822.

(20) (a) *Fluorinated Pharmaceuticals: Advances in Medicinal Chemistry*, (E. D. Westwell Ed.), **2015**, Future Science Ltd., London; (b) C. Wang, L. Chen, Y. Sun, W. Guo, A. K. Taouil, J. Ojima, Design, synthesis and SAR study of Fluorine-containing 3rd-generation toxoids, *Bioorg. Chem.* **2022**, *119*, 105578; (c) M. Rull, M. Cipolloni, M. Catto, C. Colliva, D. V. Miniero, T. Latronico, M. de Candia, T. Benicchi, A. Linusson, N. Giacche, C. D. Altomare, L. Pisani, Probing Fluorinated Motifs onto Dual AChE-MAO B Inhibitors: Rational Design, Synthesis, Biological Evaluation, and Early-ADME Studies, *J. Med. Chem.* **2022**, 3962; (d) P. K. Mykhailink, Fluorine-Containing Prolines: Synthetic Strategies, Applications, and Opportunities, *J. Org. Chem.* **2022**, *11*, 6961; (e) E. A. Fayed, N. A. Gohar, A. H. Bayoumi, Y. A. Ammar, Novel fluorinated pyrazole-based heterocycles scaffold: cytotoxicity, in silico studies and molecular modelling targeting double mutant EGFR L858R/T790M as antiproliferative and apoptotic agents, *Med. Chem. Res.* **2023**, *32*, 369.

(21) (a) Z. Nairoukh, M. Wollenburg, C. Schleppehorst, K. Bergander, F. Glorius, The Formation of All-Cis-(Multi)Fluorinated Piperidines by a Dearomatization–Hydrogenation Process, *Nat. Chem.* **2019**, *11*, 264; (b) A. M. Remete, M. Nonn, J. Escorihuela, S. Fustero, L. Kiss, Asymmetric Methods for Carbon-Fluorine Bond Formation, *Eur. J. Org. Chem.* **2021**, 5946; (c) S. Liu, B. Q. Zhang, W. Y. Xiao, Y. L. Li, J. Deng, Recent Advances in Catalytic Asymmetric Syntheses of Functionalized Heterocycles via Halogenation/Chalcogenation of Carbon-Carbon Unsaturated Bonds, *Adv. Synth. Cat.* **2022**, *364*, 3974; (d) M. Zhou, Z. Feng, X. Zhang, Recent advances in the synthesis of fluorinated amino acids and peptides, *Chem. Commun.* **2023**, *59*, 1434.

(22) T. Wu, G. Yin, G. Liu, Palladium-Catalyzed Intramolecular Aminofluorination of Unactivated Alkenes, *J. Am. Chem. Soc.* **2009**, *131*, 16354.

(23) C. Hou, P. Chen, G. Liu, Enantioselective Palladium(II)-Catalyzed Oxidative Aminofluorination of Unactivated Alkenes with Et₄NF·3HF as a Fluoride Source, *Angew. Chem., Int. Ed.* **2020**, *59*, 2735.

(24) T. Wu, J. Cheng, P. Chen, G. Liu, Regioselective Palladium-Catalyzed Intramolecular Oxidative Aminofluorination of Unactivated Alkenes, *Chem. Commun.* **2013**, *49*, 8707.

(25) (a) B. Šmit, P. B. Stanić, N. Janković, Selenocyclization by formation of carbon-nitrogen bonds, *Curr. Org. Synth.* **2022**, *19*, 293; (b) S. Devi, J. Kiran, D. Wadhwa, J. Sindhu, Electroorganic Synthesis: An Environmentally Benign Alternative for Heterocycle Synthesis, *Org. Biomol. Chem.* **2022**, *20*, 5163.

(26) B. Šmit, R. Z. Pavlović, Three-step synthetic pathway to fused bicyclic hydantoins involving a selenocyclization step, *Tetrahedron* **2015**, *71*, 1101.

(27) B. Šmit, M. Rodić, R. Z. Pavlović, Synthesis of angularly fused (homo)triquinane type hydantoins as precursors of bicyclic α -prolines, *Synthesis-Stuttgart* **2016**, *48*, 387.

(28) B. M. Šmit, R. Z. Pavlović, D. A. Milenković, Z. S. Marković, Mechanism, kinetics and selectivity of selenocyclization of 5-alkenyl hydantoins: experimental and computational study, *Beilstein J. Org. Chem.* **2015**, *11*.

- (29) K. M. Mennie, S. M. Banik, E. C. Reichert, E. N. Jacobsen, Catalytic Diastereo- and Enantioselective Fluoroamination of Alkenes, *J. Am. Chem. Soc.* **2018**, *140*, 4797.
- (30) V. V. Zhdankin, K. Muniz, Editorial for the Special Issue on Hypervalent Iodine Reagents, *J. Org. Chem.* **2017**, *82*, 11667.
- (31) A. Yoshimura, V. V. Zhdankin, Advances in Synthetic Applications of Hypervalent Iodine Compounds, *Chem. Rev.* **2016**, *116*, 3328.
- (32) Q. Wang, W. Zhong, X. Wei, M. Ning, X. Meng, Z. Li, Metal-Free Intramolecular Aminofluorination of Alkenes Mediated by PhI(OPiv)₂/Hydrogen Fluoride-Pyridine System, *Org. Biomol. Chem.* **2012**, *10*, 8566.
- (33) G. Q. Liu, Y. M. Li, Regioselective (Diacetoxyiodo)Benzene-Promoted Halocyclization of Unfunctionalized Olefins, *J. Org. Chem.* **2014**, *79*, 10094.
- (34) S. V. Kohlhepp, T. Gulder, Hypervalent Iodine(III) Fluorinations of Alkenes and Diazo Compounds: New Opportunities in Fluorination Chemistry, *Chem. Soc. Rev.* **2016**, *45*, 6270.
- (35) W. Kong, P. Feige, T. De Haro, C. Nevado, Regio- and Enantioselective Aminofluorination of Alkenes, *Angew. Chem., Int. Ed.* **2013**, *52*, 2469.
- (36) S. Suzuki, T. Kamo, K. Fukushi, T. Hiramatsu, E. Tokunaga, T. Dohi, Y. Kita, N. Shibata, Iodoarene-Catalyzed Fluorination and Aminofluorination by an Ar-I/HF·pyridine/MCPBA System, *Chem. Sci.* **2014**, *5*, 2754.
- (37) W. Yuan, K. J. Szabó, Catalytic Intramolecular Aminofluorination, Oxyfluorination, and Carbofluorination with a Stable and Versatile Hypervalent Fluoroiodine Reagent, *Angew. Chem. Int. Ed.* **2015**, *54*, 8533.
- (38) R. A. Holton, H. B. Kim, C. Somoza, F. Liang, R. J. Biediger, P. D. Boatman, M. Shindo, C. C. Smith, S. Kim, H. Nadizadeh, Y. Suzuki, C. Tao, P. Vu, S. Tang, P. Zhang, K. K. Murthi, L. N. Gentile, J. H. Liu, First Total Synthesis of Taxol. 2. Completion of the C and D Rings, *J. Am. Chem. Soc.* **1994**, *116*, 1599.
- (39) I. V. Escamilla, L. F. R. Ramos, J. S. Escalera, A. Á. Hernández, Studies on the Deprotection of Triisopropylsilylarylacetylene Derivatives, *J. Mex. Chem. Soc.* **2011**, *55*, 133.
- (40) G. Pandey, G. Lakshmaiah, Ag(I)F as One Electron Oxidant for Promoting Sequential Double Desilylation: An Ideal Approach to Non-Stabilized Azomethine Ylides for the Rapid Construction of I-Azabicyclo (m:3:0) Alkanes, *Tetrahedron Lett.* **1993**, *34*, 4861.
- (41) B. H. Rotstein, N. A. Stephenson, N. Vasdev, S. H. Liang, Spirocyclic Hypervalent Iodine(III)-Mediated Radiofluorination of Non-Activated and Hindered Aromatics, *Nat. Commun.* **2014**, *5*, 1.
- (42) S. Izquierdo, S. Essafi, I. Del Rosal, P. Vidossich, R. Pleixats, A. Vallribera, G. Ujaque, A. Lledós, A. Shafir, Acid Activation in Phenyliodine Dicarboxylates: Direct Observation, Structures, and Implications, *J. Am. Chem. Soc.* **2016**, *138*, 12747.
- (43) H. M. Lovick, F. E. Michael, Metal-Free Highly Regioselective Aminotrifluoroacetoxylation of Alkenes, *J. Am. Chem. Soc.* **2010**, *132*, 1249.

- (44) I. V. Alabugin, K. Gilmore, Finding the Right Path: Baldwin “Rules for Ring Closure” and Stereoelectronic Control of Cyclizations, *Chem. Commun.* **2013**, *49*, 11246.
- (45) F. Mocci, G. Uccheddu, A. Frongia, G. Cerioni, Solution Structure of Some Λ^3 Iodanes: An ^{17}O NMR and DFT Study, *J. Org. Chem.* **2007**, *72*, 4163.
- (46) K. Wang, X. Cai, W. Yao, D. Tang, R. Kataria, H. S. Ashbaugh, L. D. Byers, B. C. Gibb, Electrostatic Control of Macrocyclization Reactions within Nanospaces, *J. Am. Chem. Soc.* **2019**, *141*, 6740.
- (47) Y. Pocker, R. F. Buchholz, Electrostatic Catalysis by Ionic Aggregates. I. The Ionization and Dissociation of Trityl Chloride and Hydrogen Chloride in Lithium Perchlorate-Diethyl Ether Solutions, *J. Am. Chem. Soc.* **1970**, *92*, 2075.
- (48) M. Lj. Mihailović, R. Vukićević, S. Konstantinović, S. Milosavljević, G. Schroth, Intramolecular Cyclization of Some Unsaturated Alcohols by Means of Thallium Triacetate, *Liebigs Ann. Chem.* **1992**, *1992*, 305.
- (49) M. Ochiai, T. Sueda, K. Miyamoto, P. Kiprof, V. V. Zhdankin, Trans Influences on Hypervalent Bonding of Aryl Λ^3 -Iodanes: Their Stabilities and Isodesmic Reactions of Benziodoxolones and Benziodazolones, *Angew. Chem., Int. Ed.* **2006**, *45*, 8203.
- (50) P. K. Sajith, C. H. Suresh, Quantification of the Trans Influence in Hypervalent Iodine Complexes, *Inorg. Chem.* **2012**, *51*, 967.
- (51) J. I. Seeman, The Curtin-Hammett Principle and the Winstein-Holness Equation: New Definition and Recent Extensions to Classical Concepts, *J. Chem. Educ.* **1986**, *63*, 42.
- (52) T. L. Macdonald, N. Narasimhan, Nucleophilic Substitution of Alkyl iodides via Oxidative Ligand Transfer, *J. Org. Chem.* **1985**, *50*, 5000.
- (53) I. V. Alabugin, T. A. Zeidan, Stereoelectronic Effects and General Trends in Hyperconjugative Acceptor Ability of σ Bonds, *J. Am. Chem. Soc.* **2002**, *124*, 3175.
- (54) B. Harris, G. P. Savage, J. M. White, Hyperconjugation Involving Strained Carbon-Carbon Bonds. Application of the Variable Oxygen Probe to Ester and Ether Derivatives of Cubylmethanol, *Org. Biomol. Chem.* **2013**, *11*, 3151.
- (55) L. Zhiquan, H. Xie, S. E. Border, J. Gallucci, R. Z. Pavlović, J. D. Badjić, Stimuli-Responsive Molecular Capsule with Switchable Dynamics, Chirality, and Encapsulation Characteristics, *J. Am. Chem. Soc.* **2018**, *140*, 11091.
- (56) R. Z. Pavlović, L. Zhiquan, M. Guney, H. Xie, R. Lalissee, R. Hopf, J. Gallucci, C. Hadad, C. Moore, J. D. Badjić, Multivalent C–H \cdots Cl/Br–C Interactions Directing the Resolution of Dynamic and Twisted Capsules, *Chem. Eur. J.* **2019**, *25*, 13124.
- (57) R. Z. Pavlović, R. F. Lalissee, A. L. Hansen, C. A. Waudby, Z. Lei, M. Güney, X. Wang, C. M. Hadad, J. D. Badjić, From Selection to Instruction and Back: Competing Conformational Selection and Induced Fit Pathways in Abiotic Hosts, *Angew. Chem., Int. Ed.* **2021**, *60*, 19942.

(58) M. Kandrnálová, Z. Kokan, V. Havel, M. Nečas, V. Šindelář, Hypervalent Iodine Based Reversible Covalent Bond in Rotaxane Synthesis, *Angew. Chem., Int. Ed.* **2019**, *58*, 18182.